

Conformation-opioid activity relationships of bicyclic guanidines from 3D similarity analysis

Karina Martínez-Mayorga,^{a,*} Jose L. Medina-Franco,^a Marc A. Giulianotti,^a Clemencia Pinilla,^b Colette T. Dooley,^a Jon R. Appel^b and Richard A. Houghten^{a,b}

^aTorrey Pines Institute for Molecular Studies, 5775 Old Dixie Highway, Fort Pierce, FL 34946, USA

^bTorrey Pines Institute for Molecular Studies, 3550 General Atomics Court, San Diego, CA 92121, USA

Received 27 February 2008; revised 19 April 2008; accepted 23 April 2008

Available online 27 April 2008

Abstract—Conformation of bicyclic guanidines with kappa-opioid receptor activity derived in our laboratory from a positional scanning synthetic combinatorial library is presented in this work. We propose a common bioactive conformation and putative pharmacophoric features by means of 3D similarity methods. Our ‘Y’ shape molecular binding model explains structure–activity relationships and suggests that the guanidine functionality and a 4-methoxybenzyl group may be involved in key interactions with the receptor. Comparison of our model with known opiates suggest a similar binding mode showing that the bicyclic guanidines presented in this work are suitable scaffolds for further development of new opioid receptors ligands.

© 2008 Elsevier Ltd. All rights reserved.

1. Introduction

Opioid receptors are membrane proteins that belong to the G-protein coupled receptors (GPCR) superfamily. The three opioid receptors in the central nervous system and periphery are mu (μ), kappa (κ) and delta (δ).^{1,2} X-ray crystal structures of the prototype GPCR rhodopsin in its inactive form (dark state) were the first available.^{3,4} They have been extensively employed in experimental⁵ and computational studies.^{6,7} Moreover, their use has been expanded to other GPCR's, such as in cases of opioid receptors where the corresponding coordinates derived from homology modeling have been published.⁸

Key contacts for molecular recognition in opioids are known based on experimental techniques, namely site-directed mutagenesis, chimeric, and affinity labeling studies.⁹ Mutagenesis has revealed that binding occurs within conserved regions of the transmembrane helices, specifically the interactions between an amine and phenolic group of the ligand with residues Asp138 and His291, respectively. These interactions form a region called ‘message’ and this region is common to both

selective and non-selective opioid ligands (see Kane et al.⁹ for an explanation of the ‘message–address’ concept). On κ and δ opioids the ‘address’ region has been shown to confer selectivity. An extra positively charged guanidinyl group on the ligand is thought to form a salt bridge with Glu297, an interaction that is considered as the basis of κ selectivity. A hydrophobic group (indole for instance) in the address moiety confers selectivity to the δ opioid receptor. The prototypical μ -opiate morphine, however, lacks an address moiety. A model derived to explain the basis for its selectivity suggested the interaction of the amine, phenolic ring and 6 α -hydroxyl group with Asp147, Tyr299, and Cys321, respectively, as the key features.¹⁰ The interactions that confer selectivity to nonopiate ligands are not well understood. One of the issues is the high flexibility that they show, which in some cases cause speculation on the binding site.⁹

Positional scanning-synthetic combinatorial libraries (PS-SCL) have been used to successfully identify active molecules for a variety of biological targets.^{11–13} In the case of opioid receptors highly active peptides^{14,15} and peptidomimetics have been identified.¹⁵ Based on this strategy a set of bicyclic guanidines (BCG) were found with a range of activity at the κ -opioid receptor (from $IC_{50} = 37$ nM to $>10,000$ nM).^{11,13} The binding modes of these BCGs and comparison with binding modes of

Keywords: Molecular similarity; Structure–activity relationships; Opioid receptor ligands; Multi-fusion similarity maps; Mixture-based combinatorial libraries.

* Corresponding author. Tel.: +1 772 462 0892; fax: +1 772 462 0886; e-mail: kmartinez@tpims.org

known opiates may help in the design of new opioid ligands.

Ligand-based computational methods have been shown to be useful tools for exploring binding modes.¹⁶ Rapid overlay of chemical structures (ROCS) is a 3D shape-based method used to superimpose conformers of a candidate molecule with a query molecule. ROCS maximizes the shared volume between each conformer in a database against the query.¹⁷ Taking into account the chemical nature of the molecule (position of heteroatoms) enhances the results. When the conformation of a compound in the binding site is known, obtained by X-ray crystallography or NMR for instance, it may be used as the reference conformation.¹⁸ In certain cases a low energy conformation is considered as a starting point.¹⁷ However, there are several examples, as in the case of this study, where the bioactive conformation is unknown. Here, we employed ROCS of BCGs to derive a molecular binding model. Structural modifications based on the 3D shape comparison with known opiates are also suggested.

2. Results and discussion

2.1. 3D similarity analysis

Chemical structures and the corresponding IC₅₀ values for the BCGs used to develop the binding model are summarized in Table 1. These molecules were identified from a PS-SCL.¹¹ A short description of the combinatorial and synthetic methodology as well as the biological assay employed is described in Section 4.2. Generation of the conformer distribution was performed using OMEGA.¹⁹ For 3D shape comparisons the most active molecules (**1**, **2** in Table 1) were selected as queries, and will be called q1 and q2, respectively. The first step consisted in selecting the conformations of the queries. Instead of choosing conformations at random or the ones with lowest energy, the conformation of the query that showed the best correlation between similarity (combo score: shape + chemical nature score similarity) and activity was chosen. The selected conformations are depicted in Figure 1. The conformation of molecule **2** obtained when molecule **1** was the query was the same as the one obtained when molecule **2** was the query, and vice versa. In other words, the ‘Y’ shape conformation shown in Figure 1 was mutually obtained for **1** and **2**.

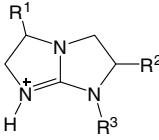
Once the optimal conformation of the queries was selected from the two most active molecules in the data set, the similarity of the remaining molecules in the database to q1 and q2 was analyzed. Results are summarized in Table 1. Figure 2 shows the corresponding multi-fusion similarity map. In this plot, the X-axis represents the *mean* combo score similarity of a given molecule to q1 and q2 while the Y-axis represents the *maximum* combo score similarity of a given molecule to either q1 or q2. A detailed description of the multi-fusion similarity maps is described elsewhere.²⁰ Data points at the top right of the plot (high *average* and high *maximum* similarity) indicate molecules that are more structurally sim-

ilar to the query set (q1 and q2 in this case) than molecules represented by data points at the lower left of the diagram (low *average* and low *maximum* combo score similarity). Closed squares represent molecules with IC₅₀ values ≤502 nM. The corresponding compound number is indicated in the plot. Open squares denote molecules with IC₅₀ > 502 nM (circles represent a second set of BCGs discussed below). As discussed above, molecules at the top right of the plot, for example, **6**, **3**, and **13** are the most structurally similar to the queries. The relative high combo score values suggest that these molecules could adopt a similar binding mode as the active molecules **1** and/or **2**. Finding active molecules (for example molecules **9** and **11**) in the region between 1.1 and 1.3 of combo score is more challenging but could be of interest because compounds with different binding modes may potentially be identified. Finally, a region that can be called ‘inactive’ for this particular analysis, is located at low *average* and low *maximum* combo score, apparently molecules in this region of the multi-fusion similarity map do not have the pharmacophoric features that drive activity of the reference compounds. It is important to note that nine out of the 12 most active molecules (compounds **1–7**, **10**, and **12–14**) have *maximum* combo score greater than 1.4. Thus 75% of the active molecules in the BCGs data set in Table 1 are similar (*maximum* combo score greater than 1.4) to the shape and chemistry of molecules **1** or **2** depicted in Figure 1. However, active molecules **8**, **9**, and **11** showed a lower 3D similarity to q1 and q2 (combo score less than 1.3 on *maximum* and *average* Figure 2).

Recently, a new set of BCGs have been published.¹³ These molecules were selected based on a computational deconvolution method. The method involved the calculation of a predicted inhibitory capacity for all 102,459 compounds in the library. Out of this large collection of compounds the computational deconvolution method retrieved five new BCGs with IC₅₀ values below 500 nM, as well as correctly predicting several inactive (IC₅₀ > 10,000 nM) BCGs. To test the model proposed in this work we computed the conformation and 3D similarity analysis of those molecules with respect to q1 and q2. Table 2 summarizes the second set of molecules evaluated here. *Mean* and *maximum* similarity of this second set of BCGs to the queries q1 and q2 are also included in Table 2 and are represented as circles in Figure 2, closed circles denote molecules with IC₅₀ < 500 nM and open circles denote molecules with IC₅₀ > 10,000 nM. It is of interest that all the active molecules from the second set of BCGs have combo score values above 1.3. This shows that these active molecules from an external set can be predicted to bind in a similar manner than the reference queries.

2.2. Structural requirements for activity

Most of the active molecules with IC₅₀ ≤ 500 nM have a 4-methoxybenzyl group at R² position, and the orientation of this group seems to be important for binding. One example is molecule **14** which is the enantiomer of the most active BCG of the series (**1**). Molecule **14** is able to adopt the ‘Y’ shape conformation, however the

Table 1. Bicyclic guanidines identified for the κ -opioid Receptor obtained from PS-SCL and the corresponding 3D similarity values


	R ¹	R ²	R ³	IC ₅₀ (nM)	3D similarity (combo score)			
					q1	q2	Max	Mean
1	S-Methyl	S-4-Methoxybenzyl	3-Cyclohexylpropyl	37	2.00	1.32	2.00	1.66
2	S-Methyl	R-4-Methoxybenzyl	2-Norbornylethyl	85	1.41	2.00	2.00	1.70
3	S-Methyl	S-4-Methoxybenzyl	2-Norbornylethyl	185	1.68	1.44	1.68	1.56
4	R-Cyclohexyl	S-4-Methoxybenzyl	2-Norbornylethyl	219	1.55	1.33	1.55	1.44
5	S-Methyl	R-4-Methoxybenzyl	1-Adamantylethyl	238	1.41	1.22	1.41	1.32
6	R-Cyclohexyl	R-4-Methoxybenzyl	2-Norbornylethyl	276	1.41	1.82	1.82	1.62
7	S-Cyclohexyl	S-4-Methoxybenzyl	4-(Me)-cyclohexylmethyl	336	1.48	1.26	1.48	1.37
8	R-Cyclohexyl	R-4-Methoxybenzyl	1-Adamantylethyl	341	1.29	1.24	1.29	1.27
9	R-Cyclohexyl	R-Isobutyl	2-Norbornylethyl	359	1.05	1.19	1.19	1.12
10	R-Cyclohexyl	R-4-Methoxybenzyl	4-(Me)-cyclohexylmethyl	362	1.43	1.59	1.59	1.51
11	R-Cyclohexyl	S-Cyclohexyl	4-(Me)-cyclohexylmethyl	365	1.11	1.18	1.18	1.15
12	S-Cyclohexyl	R-4-Methoxybenzyl	4-(Me)-cyclohexylmethyl	369	1.20	1.62	1.62	1.41
13	S-Methyl	R-4-Methoxybenzyl	4-(Me)-cyclohexylmethyl	425	1.24	1.71	1.71	1.48
14	S-Methyl	R-4-Methoxybenzyl	3-Cyclohexylpropyl	502	1.38	1.43	1.43	1.41
15	R-Cyclohexyl	S-Cyclohexyl	2-Norbornylethyl	524	1.07	1.20	1.20	1.13
16	R-Cyclohexyl	R-4-Methoxybenzyl	3-Cyclohexylpropyl	547	1.33	1.59	1.59	1.46
17	S-Cyclohexyl	S-Cyclohexyl	2-Norbornylethyl	560	1.16	1.14	1.16	1.15
18	S-Cyclohexyl	S-4-Methoxybenzyl	2-Norbornylethyl	715	1.59	1.35	1.59	1.47
19	R-Cyclohexyl	R-Isobutyl	4-(Me)-cyclohexylmethyl	738	1.05	1.23	1.23	1.14
20	R-Cyclohexyl	S-4-Methoxybenzyl	4-(Me)-cyclohexylmethyl	804	1.44	1.31	1.44	1.38
21	S-Cyclohexyl	R-Isobutyl	2-Norbornylethyl	827	1.06	1.46	1.46	1.26
22	S-Cyclohexyl	R-4-Methoxybenzyl	2-Norbornylethyl	924	1.18	1.46	1.46	1.32
23	S-Cyclohexyl	R-Isobutyl	4-(Me)-cyclohexylmethyl	999	0.94	1.30	1.30	1.12
24	R-Cyclohexyl	S-Cyclohexyl	4-(Me)-cyclohexylmethyl	1140	1.06	1.23	1.23	1.14
25	S-Cyclohexyl	R-Isobutyl	1-Adamantylethyl	1206	0.94	1.07	1.07	1.00
26	S-Cyclohexyl	S-Cyclohexyl	1-Adamantylethyl	1492	0.99	1.13	1.13	1.06
27	S-Methyl	S-4-Methoxybenzyl	1-Adamantylethyl	1532	1.48	1.20	1.48	1.34
28	S-Methyl	S-4-Methoxybenzyl	4-(Me)-cyclohexylmethyl	1568	1.56	1.39	1.56	1.47
29	R-Cyclohexyl	R-Isobutyl	1-Adamantylethyl	1747	0.97	1.05	1.05	1.01
30	R-Cyclohexyl	R-Isobutyl	3-Cyclohexylpropyl	1767	1.14	1.23	1.23	1.18
31	S-Methyl	S-Cyclohexyl	1-Adamantylethyl	1941	1.14	1.10	1.14	1.12
32	S-Methyl	R-Isobutyl	2-Norbornylethyl	2309	1.12	1.11	1.12	1.11
33	S-Methyl	S-Cyclohexyl	3-Cyclohexylpropyl	2497	1.31	1.15	1.31	1.23
34	R-Cyclohexyl	S-4-Methoxybenzyl	3-Cyclohexylpropyl	3456	1.25	1.26	1.26	1.25
35	S-Methyl	R-Isobutyl	1-Adamantylethyl	3641	0.99	0.93	0.99	0.96
36	S-Cyclohexyl	R-Isobutyl	3-Cyclohexylpropyl	3744	1.08	1.21	1.21	1.14
37	S-Cyclohexyl	S-4-Methoxybenzyl	3-Cyclohexylpropyl	3872	1.45	1.24	1.45	1.34
38	S-Methyl	S-Cyclohexyl	2-Norbornylethyl	4424	1.23	1.21	1.23	1.22
39	S-Cyclohexyl	S-Cyclohexyl	3-Cyclohexylpropyl	4482	1.24	1.14	1.24	1.19
40	S-Cyclohexyl	S-4-Methoxybenzyl	1-Adamantylethyl	4923	1.41	1.13	1.41	1.27
41	S-Cyclohexyl	R-4-Methoxybenzyl	3-Cyclohexylpropyl	5026	1.31	1.35	1.35	1.33
42	S-Methyl	S-Cyclohexyl	4-(Me)-cyclohexylmethyl	5061	1.18	1.26	1.26	1.22
43	S-Methyl	R-Isobutyl	3-Cyclohexylpropyl	5436	1.15	1.06	1.15	1.10
44	S-Methyl	R-Isobutyl	4-(Me)-cyclohexylmethyl	6477	1.10	1.32	1.32	1.21
45	R-Cyclohexyl	S-Cyclohexyl	3-Cyclohexylpropyl	>10,000	1.21	1.20	1.21	1.21
46	S-Cyclohexyl	R-4-Methoxybenzyl	1-Adamantylethyl	>10,000	1.10	1.10	1.10	1.10
47	R-Cyclohexyl	R-4-Methoxybenzyl	1-Adamantylethyl	>10,000	0.99	1.12	1.12	1.05
48	R-Cyclohexyl	S-Cyclohexyl	1-Adamantylethyl	>10,000	1.03	1.06	1.06	1.04

difference in orientation of the methoxy group seems to be responsible for the drop in activity from IC₅₀ = 37 nM (for molecule **1**) to 502 nM (for molecule **14**). It should be noted that the combo score value for molecule **14** is 1.3 when q1 is used as query. This ranks molecule **14** at the 15th position of similarity to q1 when the data are sorted by q1 value. This is remarkable because it shows that the 3D-shape similarity method em-

ployed here is able to distinguish (assign different combo score value) between enantiomers, a feature that is commonly neglected in similarity analysis. Interestingly molecule **9**, which lacks the 4-methoxybenzyl group, is more active than molecules **10**, **12**, **13**, and **14**, all of which have the 4-methoxybenzyl group in the *R* configuration. For the particular combination of substituents in molecules **12**, **13**, and **14**, it seems that the position of the

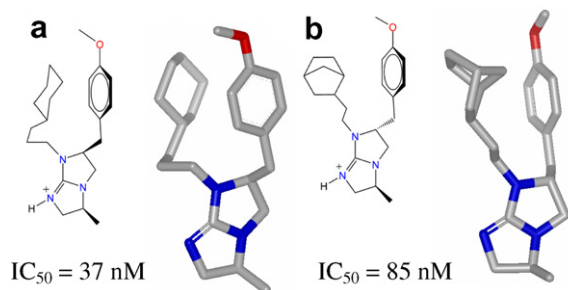


Figure 1. Molecular binding model of bicyclic guanidines: (a) **1**, and (b) **2**.

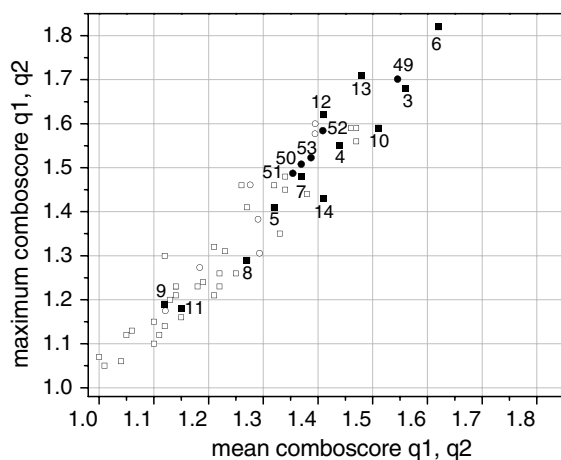


Figure 2. Multi-fusion similarity map. Data from Table 1 are represented as squares, and from Table 2 as circles. Closed shapes denote molecules with $IC_{50} \leq 500$ nM.

methoxybenzyl group is very important for activity, whereas lack of this group gives better binding affinity than having the 4-methoxybenzyl group in a misplaced orientation. Similar observations can be made for mole-

cule **11**. Actually, molecules **9** and **11** are those that have a low 3D similarity to molecules **1** and **2** (*maximum* and *average* combo score below 1.3; cf. Fig. 2). Two main features can be identified as significant for the activity of these BCGs, namely the ‘Y’ shape conformation, and the presence and orientation of the 4-methoxybenzyl group, which is influenced by the substituents at the R^1 and R^3 positions.

To illustrate the overlay of active and inactive molecules, Figure 3 depicts the best match of representative molecules from Table 2 (q2 is shown with thick lines). Figure 3a portrays the overlay of active molecules, (thin lines; $IC_{50} < 500$ nM). It is important to note that all these molecules have the same general alignment. Figure 3b depicts the overlay of inactive molecules, with $IC_{50} > 10,000$ nM. As can be seen, except for one molecule the best match found from the 3D overlay of the inactives with the query orients the 4-methoxybenzyl group in a different position than the reference. Additionally, all

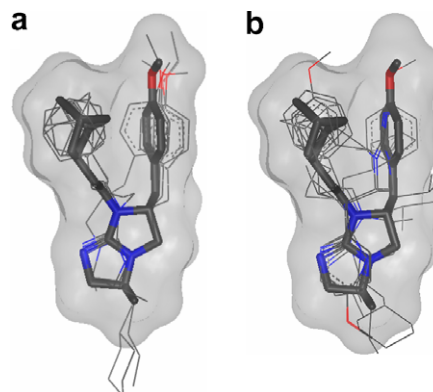
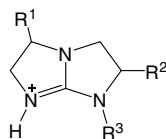


Figure 3. Overlay of BCGs from Table 2 with (a) $IC_{50} < 500$ nM, and (b) $IC_{50} > 1 \mu\text{M}$. q2 is shown as a thick stick and molecular surface.

Table 2. Bicyclic guanidines identified for κ -opioid receptor, selected from PS-SCL and computational deconvolution methods, and the corresponding 3D similarity values

	R^1	R^2	R^3	IC_{50} (nM)	3D similarity (combo score)			
					q1	q2	Max	Mean
1	S-Methyl	S-4-Methoxybenzyl	3-Cyclohexylpropyl	37	2.00	1.40	2.00	1.70
49	S-Methyl	R-4-Ethoxybenzyl	1-Adamantylethyl	151	1.39	1.70	1.70	1.55
50	S-Methyl	R-4-Ethoxybenzyl	2-Norbornylethyl	185	1.23	1.51	1.51	1.37
51	S-Ethyl	R-4-Ethoxybenzyl	2-Norbornylethyl	321	1.22	1.49	1.49	1.35
52	R-Butyl	R-4-Methoxybenzyl	2-Norbornylethyl	430	1.23	1.58	1.58	1.41
53	R-Cyclohexylmethyl	R-4-Methoxybenzyl	1-Adamantylethyl	457	1.25	1.52	1.52	1.39
54	S-Propyl	S-4-Methoxybenzyl	Cyclobutylmethyl	>10,000	1.58	1.21	1.58	1.39
55	R-Cyclohexylmethyl	S-4-Methoxybenzyl	Cyclopentylmethyl	>10,000	1.46	1.09	1.46	1.28
56	S-Isopropyl	S-4-Methoxybenzyl	Cyclopentylmethyl	>10,000	1.60	1.19	1.60	1.40
57	S-Methyl	S-Isobutyl	3-Cyclohexylpropyl	>10,000	1.38	1.20	1.38	1.29
58	S-Methyl	R-isopropyl	Cyclohexylbutyl	>10,000	1.07	1.18	1.18	1.12
59	S-Methyl	S-Methyl	1-Adamantylethyl	>10,000	1.10	1.27	1.27	1.18
60	S-Propyl	R-4-Methoxybenzyl	Cyclobutylmethyl	>10,000	1.28	1.31	1.31	1.29



the inactive compounds have an overall low combo score value.

2.3. Comparison with known opiates and suggested structural modifications

The knowledge obtained from these BCGs leads us to compare our ‘Y’ shape conformation (Fig. 1) with known opiates. The rigid structure of opiates results in a limited number of binding conformations. The minimum energy conformation of morphine, naltrindole and 5-guanidylnaltrindole (see Section 4.1) are shown in light gray in Figure 4. This minimum energy conformation was overlapped using ROCS with the ‘Y’ shape structure found for q1. It is important to point out that in this case the best match between these structures were investigated without changing the conformation of any of the molecules. Overlap of q1 with morphine, naltrindole and 5-guanidylnaltrindole is shown in Figure 4. Several structural details are remarkable. First, the orientation of the 4-methoxybenzyl group of BCG 1 lies right in the position of the hydroxyl group of the opiates. Second, the guanidine group roughly overlaps with the nitrogen atom of opiates. Third, among all the conformations that the 3-cyclohexylpropyl group (R^3 position) may adopt, it orients precisely in the same site as the remaining available group in the opiates (this can be better seen in the top view shown in Figure 4d). Finally, the methyl group at the R^1 position for the most active molecules is comparable in size to the cyclopropyl group in naltrindole and 5-guanidylnaltrindole.

As we described in the introduction, the ‘message’ region in opiates consists of key interactions between a hydroxyl group and His291 as well as an anionic region (nitrogen) and Asp138. The same interactions can potentially be occurring for the BCGs. The effect of the substitution of the 4-methoxybenzyl group for the 4-hydroxybenzyl group is currently under investigation. On the other hand, it has been shown that the selectivity of the opiates is due mainly to the group in the ‘address’ region. Because of the smaller size and higher flexibility of these BCGs, compared with opiates and other peptides²¹ which are known to bind to these GPCR’s, alter-

Table 3. Binding affinities of the two most active BCGs in the μ , κ and δ -opioid receptor

	IC ₅₀ (nM)		
	Mu	Kappa	Delta
1	421	37	5458
2	20286	85	2066

native binding modes can potentially take place. For instance the guanidine functionality may be oriented toward Glu297 (hallmark for κ selectivity,² *vide supra*). However, the excellent match (as shown in Fig. 4) of the methoxy group, the nitrogen and the potential substitution at the ‘address’ region suggest the incorporation of an indole functionality at R^3 position to induce selectivity to the δ -opioid receptor and a guanidinylnaltrindole to further enhance κ selectivity.

The binding affinity of the two most active molecules of Table 1 was tested in the μ and δ receptors (Table 3). This illustrates how the BCGs studied here are selective to κ -opioid receptor and more interestingly they show certain affinity toward μ (molecule 1) and δ (molecule 2) receptor, with IC₅₀ = 421, and 2066 nM, respectively. Molecule 1 binds with ~11 times more affinity to the κ than to the μ receptor, whereas for molecule 2 IC_{50(δ)/IC_{50(κ)} \approx 24. It is possible that the stereochemistry at the R^2 position is playing a role on the difference in selectivity. This is a promising scenario for the development of opioid ligands with different selectivity from the same scaffold. Additionally, the data shown in Table 3 reinforces the idea that these BCGs might bind with more than one orientation. Synthesis of new BCGs based on this study is in progress. Increased binding affinities will support our ‘Y’ shape model, give more structural–activity relationships insights and will encourage more refined studies for the determination of the agonist–antagonist nature of these compounds.}

3. Conclusions

3D similarity analysis and multi-fusion similarity maps lead to a ‘Y’ shape conformational model that describes

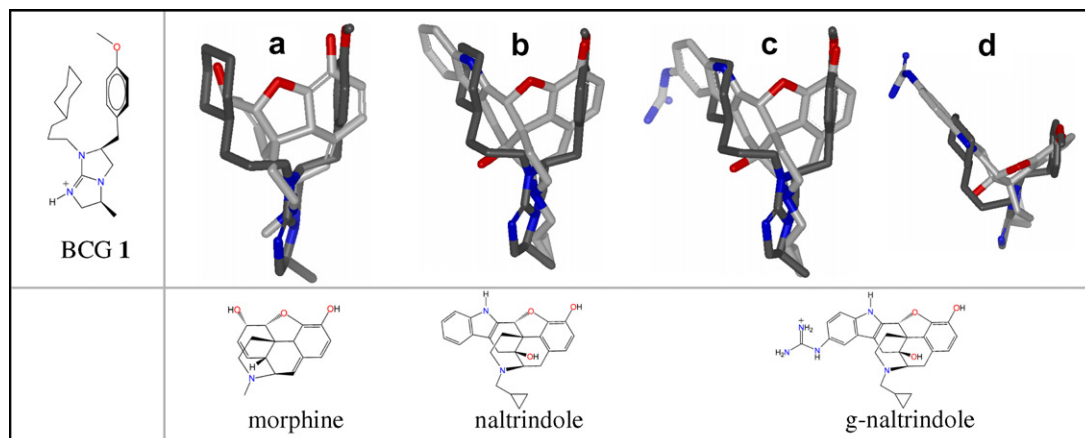


Figure 4. Overlap of BCG 1 shown in dark gray with (a) morphine, (b) naltrindole (δ antagonist) and (c) 5-guanidylnaltrindole (κ antagonist), (d) top view of (c).

the most active bicyclic guanidines studied here. Comparison with known opiates suggests pharmacophoric features involved in the binding recognition. Based on the model proposed here, structural changes are suggested to potentially increase binding affinity and selectivity of these bicyclic guanidines. Combination of ligand-based similarity methods with the structure–activity relationships accessed from combinatorial libraries is especially valuable for drug development, particularly for systems where the high resolution 3D structure of the receptor is unknown, which is the case for the vast majority of G-protein coupled receptors.

4. Methods

4.1. Computational details

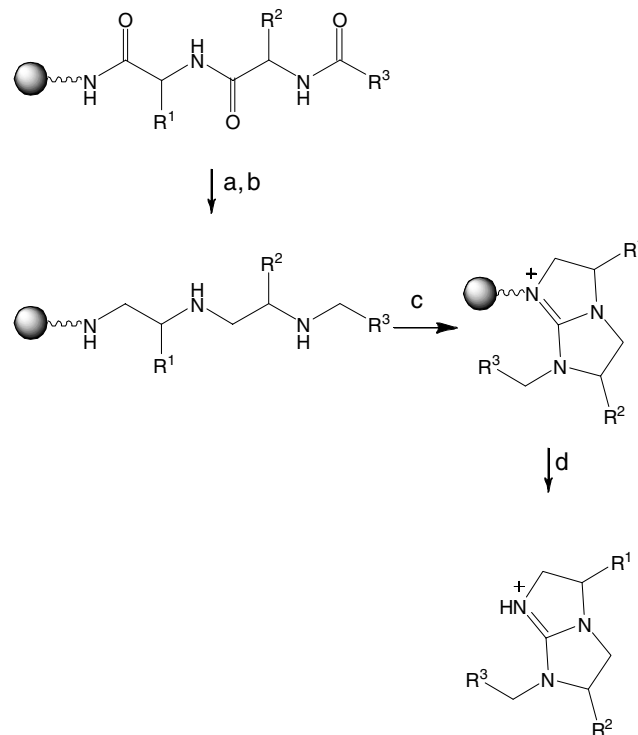
Molecules shown in Tables 1 and 2 were built and optimized using Spartan 06²² with MMFF force field. Generation of the conformers was done using OMEGA¹⁹ and employed in the 3D similarity analysis performed with ROCS.²³ The default parameters were employed throughout. VIDA was used for visualization. Data analysis was performed with Spotfire 9.1²⁴ and Origin Lab 7.²⁵

4.2. PS-SCL, synthesis, and biological assay

The conceptual and experimental framework of PS-SCL is described in detail elsewhere.^{11–13} However, this section summarizes the combinatorial chemistry strategy, solid-phase synthesis and biological assay used for the BCGs studied here.

A positional scanning-synthetic combinatorial library (PS-SCL) having three positions of diversity and composed of 102,459 bicyclic guanidines was prepared using the synthetic pathway described below. The first diversity position (R^1) is comprised of 49 different amino acids, the second (R^2) 51 amino acids and the third (R^3) 41 carboxylic acids. In this manner 141 samples are used to assess the bioactivity of 102,459 bicyclic guanidines.¹¹ Scheme 1 shows the general synthetic pathway for the solid-phase synthesis of BCGs, described elsewhere.²⁶ The first step requires the exhaustive reduction of a resin bound *N*-acylated dipeptide using borane in THF. Following treatment with thiocarbonyldiimidazole, the presence of three secondary amines allows the reaction to proceed via highly reactive intermediates to the positively charged resin-bound bicyclic guanidine. HF cleavage yields protonated trisubstituted bicyclic guanidines in good yields and high purity. The bicyclic guanidine PS-SCL was screened in a radioreceptor binding assay specific for the κ -opioid receptor. The entire library was screened at 4 $\mu\text{g}/\text{mL}$; each of the 141 samples was incubated for 2.5 h at 25 °C, with 3 nM [³H]U69,593 in a total volume of 0.65 mL of guinea pig brain homogenate.²⁷ Any sample that showed >80% inhibition was screened in a dose–response manner.

The resulting IC_{50} values were then used to choose individual bicyclic guanidines for synthesis. The selected 48 individual bicyclic guanidines had IC_{50} values ranging from 37 nM to >10,000 nM (Table 1). See Houghten



Scheme 1. Solid-phase synthesis of bicyclic guanidines from *N*-acylated dipeptides. Resin is methylbenzylamine derivatized polystyrene resin. Reagents and conditions: (a) $\text{BH}_3\text{-THF}$, $\text{B}(\text{OCH}_3)_3$, 65 °C, 72 h; (b) piperidine, 65 °C, 24 h; (c) CSIm_2 in CH_2Cl_2 , 16 h; (d) HF, anisole, 0 °C, 9 h.

et al.¹¹ for an extensive review of the results obtained from the screening of the bicyclic guanidine PS-SCL in the κ -opioid binding assay.¹¹ The second set of bicyclic guanidines (Table 2) were prepared and biologically tested in a similar manner. The selection of the second set of molecules was based on PS-SCL and computational deconvolution methods as described in Houghten et al.¹³ (vide supra). The range of activities obtained, from highly active to inactive, is typical for individual compounds synthesized based on data from the screening of a PS-SCL.

Acknowledgment

This work was supported by the State of Florida, Executive Officer of the Governor's Office of Tourism, Trade and Economic Development. The authors are also grateful to the National Institute on Drug Abuse (DA019620) and to the Multiple Sclerosis National Research Institute for partial funding. The authors acknowledge OpenEye Scientific Software, INC. for providing ROCS, OMEGA and VIDA programs.

References and notes

- Corbett, A. D.; Henderson, G.; McKnight, A. T.; Paterson, S. J. *Br. J. Pharmacol.* 147, S153.
- Stevens, W. C.; Jones, R. M.; Subramanian, G.; Metzger, T. G.; Ferguson, D. M.; Portoghese, P. S. *J. Med. Chem.* 2000, 43, 2759.

- Palczewski, K.; Kumasaka, T.; Hori, T.; Behnke, C. A.; Motoshima, H.; Fox, B. A.; Trong, I. L.; Teller, D. C.; Okada, T.; Stenkamp, R. E.; Yamamoto, M.; Miyano, M. *Science* **2000**, *289*, 739.
- Okada, T.; Sugihara, M.; Bondar, A.-N.; Elstner, M.; Entel, P.; Buss, V. *J. Mol. Biol.* **2004**, *342*, 571.
- Struts, A. V.; Salgado, G. F. J.; Tanaka, K.; Krane, S.; Nakanishi, K.; Brown, M. F. *J. Mol. Biol.* **2007**, *372*, 50.
- Martínez-Mayorga, K.; Pitman, M. C.; Grossfield, A.; Feller, S. E.; Brown, M. F. *J. Am. Chem. Soc.* **2006**, *128*, 16502.
- Zhang, Y.; DeVries, M. E.; Skolnick, J. *PLoS Comput. Biol.* **2006**, *2*, 0088.
- Pogozheva, I. D.; Przydzial, M. J.; Mosberg, H. I. *AAPS J.* **2005**, *07*, E434.
- Kane, B. E.; Svensson, B.; Ferguson, D. M. *AAPS J.* **2006**, *8*, E126.
- Kanematsu, K.; Sagara, T. *Curr. Med. Chem. CNS Agents* **2001**, *1*, 1.
- Houghten, R. A.; Pinilla, C.; Appel, J. R.; Blondelle, S. E.; Dooley, C. T.; Eichler, J.; Nefzi, A.; Ostresh, J. M. *J. Med. Chem.* **1999**, *42*, 3743.
- Pinilla, M. C.; Appel, J. R.; Borras, E.; Houghten, R. *Nat. Med.* **2003**, *9*, 118.
- Houghten, R. A.; Pinilla, C.; Giulianotti, M.; Appel, J. R.; Dooley, C. T.; Nefzi, A.; Ostresh, J. M.; Yu, Y.; Maggiora, G. M.; Medina-Franco, J. L.; Brunner, D.; Schneider, J. *J. Comb. Chem.* **2008**, *10*, 3.
- Dooley, C. T.; Chung, N. N.; Wilkes, B. C.; Schiller, P. W.; Bidlack, J. M.; Pasternak, G. W.; Houghten, R. *Science* **1994**, *266*, 2019.
- Houghten, R. A.; Dooley, C. T.; Appel, J. R. *AAPS J.* **2006**, *8*, E371.
- Stahura, F. L.; Bajorath, J. R. *Comb. Chem. High T. Scr.* **2004**, *7*, 259.
- Hawkins, P. C. D.; Skillman, A. G.; Nicholls, A. *J. Med. Chem.* **2007**, *50*, 74.
- McGaughey, G. B.; Sheridan, R. P.; Bayly, C. I.; Culbertson, J. C.; Kreatsoulas, C.; Lindsley, S.; Maiorov, V.; Truchon, J. F.; Cornell, W. D. *J. Chem. Inf. Model.* **2007**, *47*, 1504.
- OMEGA; version 2.2.1 OpenEye Scientific Software: Santa Fe, NM, USA. Available at: www.eyesopen.com.
- Medina-Franco, J. L.; Maggiora, G. M.; Giulianotti, M. A.; Pinilla, C.; Houghten, R. A. *Chem. Biol. Drug. Des.* **2007**, *70*, 393.
- Przydzial, M. J.; Pogozheva, I. D.; Bosse, K. E.; Andrews, S. M.; Sharp, T. A.; Traynor, J. R.; Mosberg, H. I. *Peptide Res.* **2005**, *65*, 333.
- Spartan06 Available at: www.wavefun.com Shao, Y. et al. *Phys. Chem. Chem. Phys.* **2006**, *8*, 3172.
- ROCS; version 2.3.1 OpenEye Scientific Software: Santa Fe, NM, USA. Available at: www.eyesopen.com.
- TIBCO Software Inc., S. U., Somerville, M. A. Available at: www.spotfire.com.
- OriginLab-TM Corporation, Version 7.5 Northampton, MA, USA. Available at: www.originlab.com.
- Ostresh, J. M.; Schoner, C. C.; Hamashin, V. T.; Nefzi, A.; Meyer, J. P.; Houghten, R. A. *J. Org. Chem.* **1998**, *63*, 8622.
- Smith, J. A. M.; Hunter, J. C.; Hill, R. G.; Hughes, J. J. *Neurochem.* **1989**, *53*, 27.